

Stress threshold for precursor decay in LiF

J. J. Dick, George E. Duvall, and J. E. Vorthman

Shock Dynamics Laboratory, Department of Physics, Washington State University, Pullman, Washington 99163

(Received 26 April 1976)

Single crystals of LiF have been mechanically shocked by projectile impact so as to produce shocks propagating in a $\langle 100 \rangle$ direction. Velocities of projectiles have been varied to produce shock pressures from 4.9 to 28.6 kbar in the LiF. Pressures were measured with thick quartz gauges after shock travel distances of approximately 3 mm. The 4.9-kbar wave was perfectly elastic. The precursor of an 8.3-kbar wave showed no attenuation, but stress relaxation occurred between precursor and plastic shock. A 10.4-kbar precursor was measurably attenuated from its impact value. These results are taken to indicate a threshold shear stress between 2.4 and 3.0 kbar for nucleation of dislocations in the shock front.

PACS numbers: 62.50.+p, 62.20.Fe

I. INTRODUCTION

It has often been noted that dislocation densities found in unshocked materials are as much as three orders of magnitude smaller than required to explain measured rates of precursor decay in plane-shock-wave experiments by conventional dislocation theory.¹⁻⁷ Three explanations of this discrepancy have been described⁷: dislocation velocities may be supersonic, multiplication of dislocations by cross glide or other processes may occur in the shock front, or dislocations may be nucleated around defects in the crystal lattice. It is implausible that dislocation velocities are sufficiently supersonic to explain the observed discrepancy, since drag forces increase at an enormous rate as the sonic limit is exceeded. The plausibility of regenerative multiplication in the shock front depends on rise time of the elastic precursor and value of the dislocation multiplication constant M .⁸ The possibility that this process is important is hard to evaluate because measured rise times are often suspect, being affected by experimental procedures as well as by material properties.

Asay *et al.*³ and Gupta *et al.*⁷ have constructed a persuasive case for the thesis that nucleation is responsible for the observed decay in lithium fluoride. In the latter paper it is shown that the strong dependence of precursor decay rate on shear stress on slip systems for $\langle 100 \rangle$ shock propagation is compatible with the theory of dislocation nucleation around impurity precipitates. In a later paper, Gupta⁹ has also shown that rate of decay varies with impact velocity in accord with the above model.

The dependence of inferred dislocation density on resolved shear stress shown in Fig. 3 of Ref. 7 suggests that for impact pressure less than approximately 10 kbar, no precursor attenuation at all should be measured in a laboratory shock experiment. This paper is a report of results obtained in experiments to test this suggestion. The necessary formalism is described in Sec. II of Ref. 7 and measuring techniques are described in Sec. III of the same paper.

II. EXPERIMENTAL DETAILS

Gupta referred to the lithium fluoride he used in measuring stress dependence of precursor decay rate as $H(\text{Ann. III})$.⁹ It was obtained from Harshaw Chemical

Co. and contained 120 ± 25 -ppm magnesium as the principal impurity (molar concentrations are used throughout). Samples were kept at 400°C for 12 h, then air quenched to room temperature. Following this they were annealed at 150°C for 70 h to encourage precipitation of magnesium fluoride. Finally, they were slowly cooled to room temperature.

The boule from which Gupta's samples were drawn was exhausted, so new samples with 120-ppm magnesium were ordered from Rosenberger at the University of Utah. These were all grown from the same starting material but were not from a single boule. Several measurements of magnesium concentration were obtained and the results are shown in Table I. Magnesium con-

TABLE I. Measurements of magnesium concentration (spectrographic analysis also detected less than 2 ppm of Si, Cu, Ca, and Al).

Specimen No.	Reported magnesium concentration, mole ppm ^a	Source
14	74 ^b	f
	158 ^c	g
15	145 ^c	g
	76, ^b 67, ^c 106 ^d	f
7	151 ^c	g
	148 ^c	g
16	148 ^c	g
	152, ^d 380 ^d	e
17	163 ^c	g
	27 ^d	h
3	76 ^b	f
	201 ^c	g
	54 ^d	h
4	73 ^b	f
	189 ^c	g

^aThis is the molar ratio of Mg to LiF in ppm.

^bAnnealed.

^cAir quenched.

^dAs-received.

^eWest Coast Technical Service, Inc., Cerritos, Calif. atomic absorption; 2-5% accuracy.

^fF. Rosenberger, Department of Physics, University of Utah; atomic absorption; 2% accuracy.

^gYield stress measurement and Ref. 10.

^hAmerican Spectrographic Laboratories, Inc., San Francisco, Calif.; spectrographic measurements; no accuracy stated.

TABLE II. Experimental parameters for precursor measurements.

Shot No.	Specimen No.	Specimen thickness (mm)	Dislocation ^a density, N_0 ($10^5/cm^2$)	Yield stress (kbar)		Projectile material	Projectile velocity (mm/ μ sec)	Calculated elastic impact pressure (kbar)	Measured precursor amplitude (kbar)
				air quenched	annealed				
75-050	14	2.55	1.6	0.105	0.395	PMMA	0.162 \pm 0.011	4.9	4.9
75-054	15	3.10	0.9	0.095	0.40	PMMA	0.270 \pm 0.029	8.25	8.3
75-060	7	2.90	2.7	0.10	0.43	PMMA	0.366 \pm 0.004	11.2	10.4
75-062	16	3.10	2.9	0.097	0.41	PMMA	0.450 \pm 0.004	13.8	12.6
75-063	17	3.16	—	0.109	0.43	Al	0.2305	19.1	14.6
75-036	3	2.76	1.9	0.14	0.39 \pm 0.04	Al	0.344 \pm 0.004	28.6	21.8
75-040	4	3.00	1.8	0.13 \pm 0.01	0.40 \pm 0.02	Al	0.343 \pm 0.002	28.6	21.85

^a Measured by counting etch pits.

concentrations were also inferred from quasistatic yield stress measurements on air-quenched samples, given in Table II, according to Fig. 1(a) of Ref. 10. Specimens 3 and 4 were treated differently from the others in two respects. They were annealed at 146°C instead of 163°C, and yield measurements were made at a strain rate of $(8.2 \pm 1.3) \times 10^{-4}/\text{sec}$ instead of $(1.6 \pm 0.5) \times 10^{-4}/\text{sec}$, which was used for the others. These two factors may account for the large values of yield stress for specimens 3 and 4. The range of concentration values is distressing. It is not certain whether it represents real variation of magnesium content within and among specimens or uncertainties in measuring methods. Except for specimens 3 and 4, concentrations inferred from yield stress are closely grouped around 150-ppm magnesium. The mean of all determinations in Table I is 132 ppm, which is within the range of Gupta's values. Whether or not there is indeed a difference is uncertain.

Another difference between our specimens and Gupta's was annealing time. His were annealed for 70 h at 150°C; ours, by accident, were annealed for 57 h. According to Ref. 7, this should have reduced annealed yield stress and precursor amplitude slightly relative to Gupta's values. The difference was thought to be inconsequential.

Experiments were conducted as described in Ref. 3, 7, and 9. Projectiles for shots 75-050, 75-054, and 75-063 were 2 ft long and more massive (11 lb) than the standard projectile, which weighs about 2 lb and is 8 in. long. Tilts at impact and precursor rise times of current output from quartz gauges are listed in Table III.

Quartz gauges were used in the shorted mode.¹¹ Three calibration shots were made at low stresses.

TABLE III. Rise time and tilt.

Shot No.	Rise time (nsec)		Tilt (mrad)
	10-90%	0-100%	
75-050	25	80	0.12
75-054	~12	27	0.44
75-060	<10	13	0.14
75-062	<9	12	0.14
75-063	10	18	0.34
75-036	9	11	0.24
75-040	4	6	0.3

Current coefficients derived from initial pressure jumps are shown in Fig. 1 and compared with values reported by Hayes and Gupta.¹² The ramping correction determined in these experiments was $(26 \pm 1)\%$ instead of 40% as reported by Hayes and Gupta. No significant difference was apparent in the three experiments. Deficiencies of shorted quartz gauges are discussed elsewhere.^{12,13} They respond quickly to changes in p_x and are accurate and reliable for a short time after first response.

III. EXPERIMENTAL RESULTS

Quartz current profiles, converted to interface pressure p_x , are shown in Fig. 2. The profile from shot 75-050 appears to be absolutely elastic with amplitude equal to the calculated elastic impact amplitude. The error assignable to the amplitude measurement can be inferred from Fig. 1. Resolved shear stress in this experiment is 1.4 kbar, which is well below threshold values indicated in Ref. 7. The anticipated rate of decay of precursor in this experiment, assuming that no multiplication is occurring, can be calculated from Eqs. (2), (4), (5), (9), and (10) of Ref. 7. For a dislocation density of $1.6 \times 10^5/cm^2$, they give a precursor decay rate of approximately 10^{-3} kbar/mm, which would be unobservable in this experiment.

Shot 75-054, with calculated impact pressure of 8.25 kbar, has a precursor amplitude of 8.3 kbar. The two values are indistinguishable within the error of the experiment. p_x decreases with time immediately behind

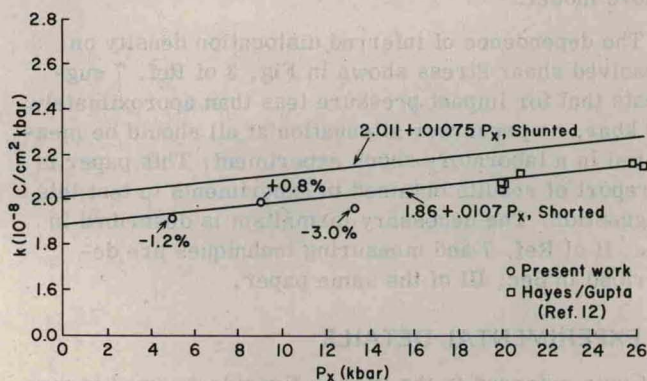


FIG. 1. Effects of pressure on the piezoelectric constants of quartz gauges.

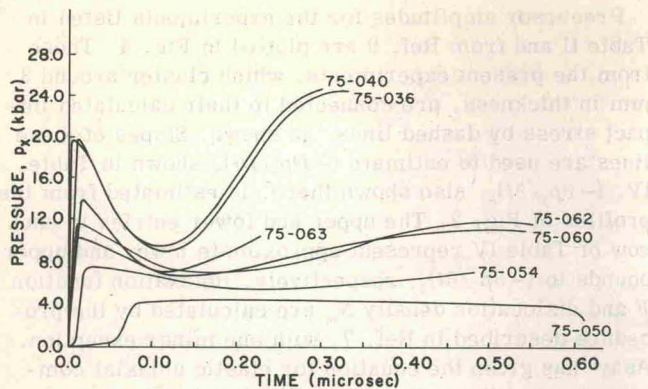


FIG. 2. Effects of impact stress on pressure-time profiles in LiF; shot numbers refer to entries in Tables II-IV.

the precursor maximum. This may arise from cross-glide multiplication of existing dislocations. Equation (5) of Ref. 9 is the constitutive relation derived for these materials. Combining this with Eqs. (2) and (13) of Ref. 7, we obtain the equation

$$\dot{N}_m = \pm \frac{3M}{C_{11} - C_{12}} \left(\dot{p}_x + \frac{C_{11}}{V} \dot{V} \right), \quad (1)$$

where $\dot{V} \equiv dV/dt$, etc., and $V = 1/\rho$ is the specific volume. The ambiguity of sign in Eq. (1) arises from the usually ignored fact that the Orwan relation, Eq. (5) of Ref. 7, involves the absolute value of the plastic strain rate. The sign in Eq. (1) is to be taken so that \dot{N}_m is positive.

In Fig. 3 are shown, with exaggerated curvature, curves of uniaxial elastic compression, OAB, and curves of quasistatic uniaxial elastic-plastic compression, OANC. For a shock of final amplitude p_x^D , the locus of (p_x, V) states followed by a mass element for a steady-state shock is the sequence of two straight lines, OA and AD. For a transient condition in which the elastic precursor amplitude is at P, the locus of states from P to the final state D is bounded by curve AB and the line AD.¹⁴ Its path, PRD, cannot be described without solving the flow equations. If PR lies along AB, $\dot{p}_x V/\dot{V} = -C_{11}$ and \dot{N}_m vanishes. Since the locus PRD is not known, we cannot relate \dot{N}_m to \dot{p}_x directly. We can, however, obtain an upper bound for total multiplication from precursor to the minimum in p_x . Assume M , C_{11} , and C_{12} to be constant in Eq. (1) and integrate from precursor to minimum. Then

$$\Delta N_m = \pm \frac{3M}{C_{11} - C_{12}} \left[\Delta p_x + C_{11} \ln \left(\frac{V_m}{V_e} \right) \right],$$

where Δp_x and $V_m - V_e$ are changes in p_x and V over the specified interval. V_e is known from the elastic relation; V_m is not known, but it is greater than the value of V at N on the plastic compression curve. Call this V_N , then

$$\Delta N_m < - \frac{3M}{C_{11} - C_{12}} \left[\Delta p_x + C_{11} \ln \left(\frac{V_N}{V_e} \right) \right]. \quad (2)$$

Suppose that APB is a curve of constant modulus, C_{11} , and ANC is of constant modulus $K = \frac{1}{3}(C_{11} + 2C_{12})$. ANC is offset vertically from the hydrostat by $p_x^A(1 - K/C_{11})$,

where p_x^A is the static HEL. Pressure on the hydrostat at volume V_e is Kp_x^e/C_{11} ; therefore,

$$p_x^G = \frac{K}{C_{11}} p_x^e + p_x^A \left(1 - \frac{K}{C_{11}} \right). \quad (3)$$

Also,

$$p_x^N - p_x^G = - \int_{V_e}^{V_N} K \frac{dV}{V} = -K \ln(V_N/V_e), \quad (4)$$

and

$$\Delta p_x = p_x^N - p_x^e. \quad (5)$$

Combining Eqs. (2)-(5) gives

$$\Delta N_m < \frac{2M}{K} (p_x^N - p_x^A) < \frac{2M}{K} p_x^N. \quad (6)$$

The difference, $p_x^e - p_x^N$, does not enter explicitly into Eq. (6). This upper-limit estimate for ΔN_m depends only on the minimum in the $p_x(t)$ profile. It is evident from Fig. 2 that p_x^N does not vary by more than a factor of 2 among all the shots recorded. One would expect the number of dislocations generated by cross glide to be much greater for shot 75-040 than for shot 75-054. What probably happens is that the stress path, PRD in Fig. 3, follows the elastic curve OAB much more closely in small-amplitude shots than in large-amplitude shots. This would cause the minimum in p_x to occur at larger V , so ΔN_m is much less than the upper bound in shot 75-054; whereas in shot 75-050 the upper bound may be a reasonable estimate.

For lithium fluoride, $M \approx 3 \times 10^9/\text{cm}^2$ and $K = 698$ kbar.¹⁵ With $p_x^N = 6$ kbar, $\Delta N_m \lesssim 1.55 \times 10^8/\text{cm}^2$. From Fig. 3 one might infer that substitution of V_N for V_m is a very bad approximation. Since the compression curves are quite straight, the errors are much smaller than the figure suggests. The value of V_m can be determined only by integrating the flow equations or by measuring the transverse component of pressure.

Shot 75-060 is the lowest amplitude one for which unambiguous decay of the precursor was recorded. Its amplitude of 10.4 kbar is 7% smaller than the calculated impact pressure of 11.2 kbar. Since resolved shear stress on the primary slip systems is 0.219 times the

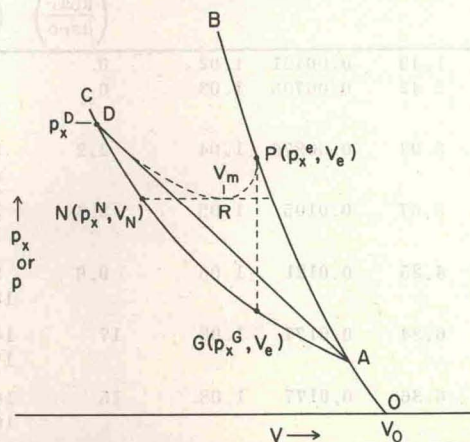


FIG. 3. Schematic representation of pressure-volume states in LiF.

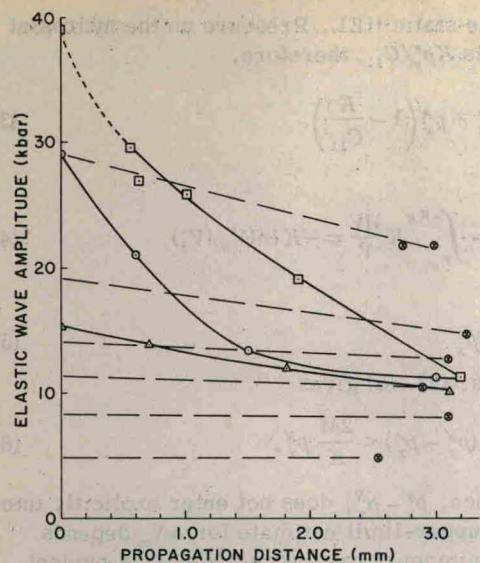


FIG. 4. Effects of impact stress and propagation distance on precursor amplitudes in LiF. □, ○, △—measurements from Ref. 9. ⊗—new results.

impact pressure, its value is 2.4 kbar for shot 75-054 and 3.0 for shot 75-060. These numbers bound the minimum value required to nucleate dislocations around magnesium fluoride precipitates in this material, according to the model proposed in Ref. 7.

Shots 75-036 and 75-040 were intended to duplicate shot 72-015 of Ref. 9. The precursor amplitude in that case was 11.4 kbar, which is but slightly more than one-half the values obtained for shots 75-036 and 75-040. The difference may arise from a difference in magnesium concentration, discussed in Sec. III. The annealing time which is slightly shorter than Gupta's Ann. III should not produce such an effect. If surface dislocations contribute to precursor decay, such an effect might be observed due to variations in surface preparation, but experiments on this point by Asay suggest that it is not important.⁵

TABLE IV. Relaxation function and dislocation parameters.

Shot No.	p_x^e (kbar)	τ^e (kbar)	e^e	C_L^2/U^2	$-\frac{Dp_x^e}{Dt}$ (kbar/ μ sec)	$-\frac{\partial p_x}{\partial t}$ (kbar/ μ sec)	F (kbar/ μ sec)	$N\bar{v}$ ($\times 10^6$ /cm μ sec)	D (kbar)	\bar{v} (cm/ μ sec)	N_m (cm $^{-2}$)
75-050	4.9	1.43	0.00421	1.02	0	0	0	...	3.63	0.0256	N_f^e
75-054	8.3	2.42	0.00705	1.03	0	4 ^a 14 ^b	0	...	3.68	0.0715	N_f^e
75-060	10.4	3.03	0.00876	1.04	2.2	22 ^a 43 ^b	3.67 2.81	0.583 0.446	3.96	0.0888	0.657×10^7 0.502×10^7
75-062	12.6	3.67	0.0105	1.05	2.4	22 ^a 50 ^b	3.95 2.56	0.625 0.405	3.77	0.117	0.534×10^7 0.346×10^7
75-063	14.6	4.25	0.0121	1.06	9.6	89 ^a 120 ^b	15.2 13.4	2.41 2.13	3.96	0.129	1.87×10^7 1.65×10^7
75-036	21.8	6.34	0.0177	1.08	17	140 ^a 170 ^b	25.2 22.7	4.00 3.59	3.59	0.186	2.15×10^7 1.93×10^7
75-040	21.85	6.36	0.0177	1.08	15	140 ^a 160 ^b	20.8 19.2	3.31 3.05	3.68	0.184	1.80×10^7 1.66×10^7

^{a,b} These are approximate lower and upper limits for $(-\partial p_x/\partial t)_h$.

Precursor amplitudes for the experiments listed in Table II and from Ref. 9 are plotted in Fig. 4. Those from the present experiments, which cluster around 3 mm in thickness, are connected to their calculated impact stress by dashed lines, as shown. Slopes of these lines are used to estimate $(-Dp_x^e/Dt)$, shown in Table IV. $(-\partial p_x/\partial t)_h$, also shown there, is estimated from the profiles of Fig. 2. The upper and lower entries in each row of Table IV represent approximate lower and upper bounds to $(-\partial p_x/\partial t)_h$, respectively. Relaxation function F and dislocation density N_m are calculated by the procedure described in Ref. 7, with one minor exception. Asay⁵ has given the equation for elastic uniaxial compression in lithium fluoride to the third order in strain as

$$p_x^e = C_{11}^s e(1 + \alpha e), \quad (7)$$

where $e = 1 - \rho_0/\rho$, C_{11}^s is an adiabatic elastic modulus, and $\alpha = 4.71$ is a dimensionless constant. With the definitions

$$C_L^2 = \left(\frac{\partial p_x^e}{\partial \rho} \right)_s \left(\frac{\rho}{\rho_0} \right)^2,$$

$$U^2 = V_0^2 [p_x^e / (V_0 - V)],$$

it is readily seen from Eq. (7) that

$$C_L^2/U^2 = 1 + \alpha e + O(e^2).$$

Then to the second order in e ,

$$F = 2(1 + \alpha e) \left(-\frac{Dp_x^e}{Dt} \right) - \alpha e \left(-\frac{\partial p_x}{\partial t} \right)_h. \quad (8)$$

Inferred dislocation density N_m is entered in the last column of Table IV. Upper and lower entries in each row show the effects of uncertainties in $(-\partial p_x/\partial t)_h$. If this derivative were set to zero, values of N_m in the last three rows would approximately double. All in all, values of N_m given in Table IV may be reliable within a factor of ~ 2 . The principal uncertainty is probably \bar{v} . Even for shot 75-060, for which precursor decay is

^c Values of dislocation density, for the unshocked material, inferred from etch pit counts are given in Table II.

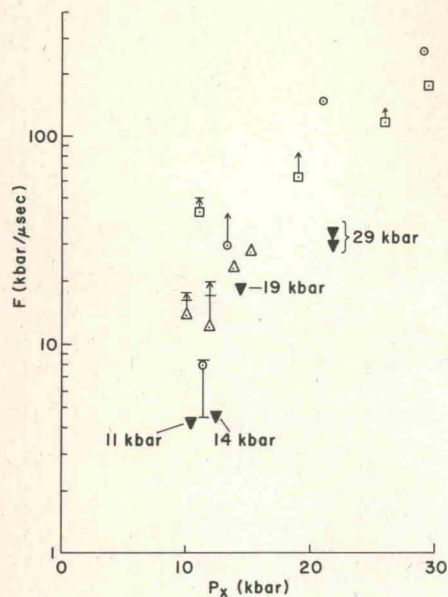


FIG. 5. Relaxation functions derived from precursor decay in LiF. \square , \circ , \triangle —from Ref. 9. ∇ —new results; pressures indicate elastic impact amplitude.

just detectable, N_m exceeds N_0 (Table II) by about 20 times, which exceeds possible errors in N_m .

Values of relaxation function F and dislocation density N_m for both these and Gupta's measurements⁹ are plotted in Figs. 5 and 6. The values reported here for impact pressures of 11.2, 13.8, and 19.1 kbar fit well with Gupta's results; the 28.6-kbar points are significantly lower, corresponding to large values of the precursor amplitude.

IV. DISCUSSION

Experiments reported here show more clearly than previous work the existence of a threshold for precursor decay in lithium fluoride and the inability of grown-in dislocations to explain rapid precursor decays observed in these and earlier experiments. The 8-kbar shot (75-054) illustrates the thesis suggested by Johnson and Rohde in their study of twinning¹⁶: no deformation mechanism which depends on plastic strain following the precursor can contribute to precursor decay. Elastic behavior recorded in shot 75-050 shows that even when rise time is very long, regenerative multiplication in the elastic shock front is insufficient to significantly modify precursor decay.

Failure of shots 75-036 and 75-040 to reproduce the nominally equivalent shot in Ref. 7 is disturbing. The difference might be due to surface preparation, but it seems more likely that it results from larger magnesium concentration. It might also be due to the presence of other impurities whose effects have been disregarded. This sensitivity of dislocation processes to small changes in impurity content was presaged by Asay *et al.*³ If such sensitivities exist in other materials, serious questions must be raised about the validity of inferences drawn about dislocation behavior from mechanical measurements on material in which impurities are but poorly known.

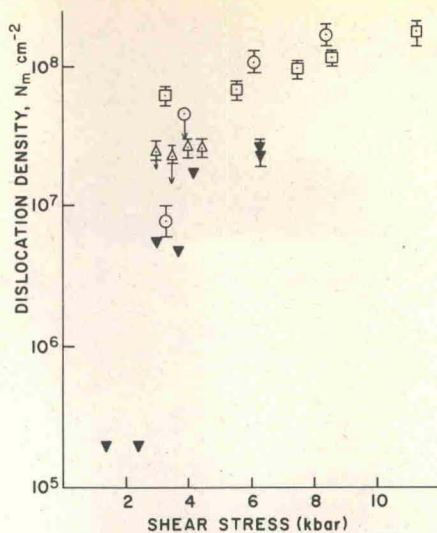


FIG. 6. Dislocation densities derived from precursor decay in LiF. \square , \circ , \triangle —from Ref. 9. ∇ —new results.

Control and measurement of material impurities certainly represent the greatest barriers to good analytical experiments of the kind attempted here and in earlier related work. In the particular case of magnesium-doped lithium fluoride, yield stress of air-quenched material may be the best indicator of concentration, but the amount of work done on this to date is not enough to provide great assurance of its reliability.

ACKNOWLEDGMENT

The authors indebted to Dr. Y. M. Gupta of Standard Research Institute for advice received in the course of this work and to P. M. Bellamy of Washington State University for assistance in the experiments. They are grateful for financial support received from the Division of Materials Research, National Science Foundation, Grant No. DMR72-03171 A02.

- ¹J.N. Johnson, O.E. Jones, and T.E. Michaels, *J. Appl. Phys.* **41**, 2330 (1970).
- ²J.N. Johnson and L.M. Barker, *J. Appl. Phys.* **40**, 4321 (1969).
- ³J.R. Asay, G.R. Fowles, G.E. Duvall, M.H. Miles, and R.F. Tinder, *J. Appl. Phys.* **43**, 2132 (1972).
- ⁴O.E. Jones and J.D. Mote, *J. Appl. Phys.* **40**, 4920 (1969).
- ⁵J.R. Asay, Ph.D. thesis (Washington State University, 1971) (unpublished).
- ⁶P.P. Gillis, K.G. Hoge, and R.J. Wasley, *J. Appl. Phys.* **42**, 2145 (1971).
- ⁷Y.M. Gupta, G.E. Duvall, and G.R. Fowles, *J. Appl. Phys.* **46**, 532 (1975).
- ⁸J.J. Gilman, *J. Appl. Phys.* **36**, 2772 (1965).
- ⁹Y.M. Gupta, *J. Appl. Phys.* **46**, 3395 (1975).
- ¹⁰Y.M. Gupta and G.R. Fowles, in *Metallurgical Effects at High Strain Rates*, edited by R.W. Rohde, B.M. Butcher, J.R. Holland, and C.H. Karnes (Plenum, New York, 1973).
- ¹¹G.A. Jones and W.J. Halpin, *Rev. Sci. Instrum.* **39**, 258 (1968).
- ¹²D.B. Hayes and Y.M. Gupta, *Rev. Sci. Instrum.* **45**, 1554 (1974).
- ¹³R.A. Graham, *J. Appl. Phys.* **46**, 1901 (1975).
- ¹⁴G.W. Swan, G.E. Duvall, and C.K. Thornhill, *J. Mech. Phys. Solids* **21**, 215 (1973).
- ¹⁵J.E. Flinn, G.E. Duvall, G.R. Fowles, and R.F. Tinder, *J. Appl. Phys.* **46**, 3752 (1975).
- ¹⁶J.N. Johnson and R.W. Rohde, *J. Appl. Phys.* **42**, 4171 (1971).